Journal of Biomolecular NMR, **13:** 175–180, 1999.
KLUWER/ESCOM
© 1999 *Kluwer Academic Publishers. Printed in the Netherlands.*

A doublet-separated sensitivity-enhanced HSQC for the determination of scalar and dipolar one-bond J-couplings

Florence Cordier[a], Andrew J. Dingley[b] & Stephan Grzesiek[a,b,*]
[a]*Institute of Structural Biology, IBI-2, Forschungszentrum Jülich, D-52425 Jülich, Germany;*
[b]*Institute of Physical Biology, Heinrich-Heine-Universität, D-40225 Düsseldorf, Germany*

Received 16 September 1998; Accepted 8 October 1998

Key words: dipolar coupling, hepatitis C protease, one-bond J coupling, sensitivity enhancement

Abstract

A simple, sensitivity-enhanced HSQC experiment is described which separates the upfield and downfield components in the indirect dimension into different subspectra. The sequence is similar to the generalized TROSY scheme; however, decoupling of the X-nucleus is used during detection. A detailed analysis of relaxation effects, precision and sensitivity of the method is presented. The approach is demonstrated in a two-dimensional water flip-back ^{1}H-^{15}N HSQC which measures $^{1}J_{HN}$ splittings in isotropic and oriented samples of ubiquitin and the hepatitis C protease. The results are in excellent agreement with splittings obtained from a conventional ^{1}H-coupled HSQC.

Residual dipolar couplings in weakly aligned molecules are observable in high resolution NMR spectra in a similar way as electronically mediated J-couplings. They provide unique information on the length and orientation of the internuclear vector (Saupe and Englert, 1963; Bothner-By et al., 1981). Very weak alignment ($\sim 10^{-4}$) of macromolecules in the magnetic field has been achieved by the anisotropy of their magnetic susceptibility (Tolman et al., 1995; Tjandra et al., 1996) resulting in one-bond ^{1}H-^{15}N or ^{1}H-^{13}C dipolar couplings on the order of a few Hertz. Such small dipolar couplings have been determined with very high accuracy (Tolman and Prestegard, 1996; Tjandra et al., 1996). The recent introduction of a stronger alignment (Tjandra and Bax, 1997; Bax and Tjandra, 1997) in the presence of lipid bicelles (Ram and Prestegard, 1988; Sanders and Schwonek, 1992; Vold and Prosser, 1996) has resulted in much larger residual dipolar couplings. Therefore, less stringent conditions are placed on the precision of the coupling constant determination, and interest has shifted to simpler and more sensitive schemes.

A particularly convenient method is the separation of the data into two subspectra containing only resonances of spins where the coupling partner is in either the $|\alpha>$ or the $|\beta>$ state (Ross et al., 1996; Fäcke and Berger, 1996; Meissner et al., 1997a,b; Andersson et al., 1998a; Ottiger et al., 1998). Since the resonance is split into a doublet, the sensitivity of most of these experiments is half compared to a corresponding decoupled scheme. Sensitivity-enhanced schemes for the measurement of one-bond J-couplings have been proposed as a quantitative J-correlation, constant-time HSQC (Tolman and Prestegard, 1996) and as an HSQC with spin-state separation in the detected proton dimension (Andersson et al., 1998a). Because of long-range couplings to other protons, ^{1}H resonances are usually much broader than the resonances of ^{15}N and ^{13}C nuclei. Therefore, measurement of one-bond J-couplings is more sensitive and/or more precise during the evolution of the heteronuclei than during the evolution of protons. In this communication we show that a sensitivity-enhanced water flip-back HSQC with spin-state separation in the indirect dimension can be implemented by a modification of the TROSY sequence (Pervushin et al., 1997, 1998; Czisch and Boelens, 1998). The approach is similar to the recently proposed α/β-HSQC-α/β experiment (Andersson et al., 1998b). However, in the present scheme heteronuclear decoupling is used during the

*To whom correspondence should be addressed.

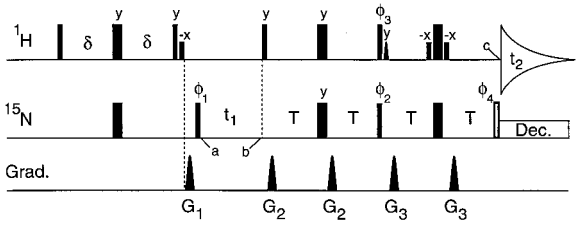

Figure 1. Pulse sequence of the DSSE-^{15}N-^{1}H-HSQC. Narrow and wide pulses denote 90° and 180° flip angles, respectively, and unless indicated otherwise the phase is x. ^{1}H and ^{15}N carrier positions are on the ^1H_2O resonance and at 116.5 ppm, respectively. Rectangular low power ^{1}H pulses are applied using $\gamma_H B_1 = 250$ Hz, the sine-bell shaped 90° pulse has a duration of 1.1 ms. All regular ^{15}N pulses are applied at an RF field strength $\gamma_N B_2 = 5.6$ kHz, whereas the ^{15}N decoupling is applied at an RF field strength of $\gamma_N B_2 = 1.25$ kHz. Delay durations: $\delta = 2.25$ ms; T = 2.7 ms. Phase cycling: $\phi_1 = x, -x$; $\phi_2 = -y$; $\phi_3 = -x$; receiver = x, −x. Gradients (sine bell shaped; 25 G/cm at center): $G_{1,2,3} = 2, 2.5$, and 0.2 ms. Application of the last ^{15}N 90° pulse (open rectangle, ϕ_4) is only necessary for the detection of the narrow component of the proton doublet (see text). In this case, ^{15}N decoupling during acquisition is omitted and separate FIDs are recorded with alternating phase settings ($\phi_4 = -x, x$) of the last ^{15}N 90° pulse.

proton evolution period and a detailed description of precision, sensitivity and relaxation artifacts is provided. The appearance of the subspectra is the same as for the in-phase/anti-phase (IPAP) ^{1}H-coupled HSQC (Ottiger et al., 1998) albeit at a signal-to-noise ratio which is increased by $\sqrt{2}$.

The scheme in Figure 1 consists of a water flip-back ^{1}H-^{15}N HSQC experiment which incorporates a double reverse INEPT scheme before the detection period, similar to the TROSY sequence (Pervushin et al., 1997) and the earlier sensitivity enhancement schemes (Palmer et al., 1991; Kay et al., 1992). Without relaxation this double reverse INEPT represents a unitary transform of the density matrix at time point *b* into another density matrix at time point *c*. The effect of this unitary transform on transverse nitrogen magnetization is most easily described by considering the transformation of the four basis vectors N_x, N_y, $2N_xH_z$, $2N_yH_z$. At time point *c*, we can restrict ourselves to the observable components of the transverse proton magnetization, i.e. H_x, H_y, $2H_xN_z$, $2H_yN_z$. In this case, the evolution from *b* to *c* is described by:

$$N_x = N_xH_\alpha + N_xH_\beta \rightarrow p * s * 2H_yN_z \quad (1a)$$

$$2N_xH_z = N_xH_\alpha - N_xH_\beta \rightarrow -p * s * H_y \quad (1b)$$

$$N_y = N_yH_\alpha + N_yH_\beta \rightarrow s^2 * H_x \quad (1c)$$

$$2N_yH_z = N_yH_\alpha - N_yH_\beta \rightarrow -2H_xN_z \quad (1d)$$

where $s = \sin(2\pi JT)$, $p = 1$ if $\phi_2 = -y$, $\phi_3 = -x$, and $p = -1$ if $\phi_2 = y$, $\phi_3 = x$. It is evident from Equation 1 that the pulse sequence between points *b* and *c* maps x- and y-components of nitrogen magnetization onto x- and y-components of proton magnetization. This behavior is analogous to the preservation of pathways and the sensitivity enhancement scheme originally proposed by Cavanagh and Rance (1990) and Palmer et al. (1991). If ^{15}N decoupling is switched on at point *c*, proton anti-phase signals in Equations 1a and 1d do not lead to observable magnetization. Since the last nitrogen 90° pulse acts only on these two signals in the pathway of Equation 1, it can also be omitted, thus leaving the signals stemming from N_x and $2N_yH_z$ as undetectable proton/nitrogen zero- and double-quantum coherences. The sign of signals from Equation 1b changes under the inversion of ϕ_2 and ϕ_3. Therefore, the observable proton signals resulting from $2N_xH_z$ and N_y magnetization can be separated by adding and subtracting two FIDs recorded with phase settings $\phi_2 = -/+y$, $\phi_3 = -/+x$, respectively.

On the other hand, transverse nitrogen magnetization with the proton in the $|\alpha>$ or in the $|\beta>$ state can be separated by the different behavior under rotations around the z-axis. This is easily seen from the representation of Equation 1 where the proton components of the transverse nitrogen magnetization are expressed in terms of polarization operators H_α and H_β (Ernst et al., 1987). A rotation by 90° around the z-axis at point *b* of the N_xH_α or N_yH_α magnetization corresponds to a rotation by 90° for proton magnetization at point *c* (assuming $p = s = 1$). The opposite rotation of proton phases is observed for magnetization originating on the N_xH_β or N_yH_β components of the nitrogen doublet. When phases ϕ_2 and ϕ_3 are inverted ($p = -1$), the inverse phase behavior results. It is therefore possible to separate the upfield and downfield components of the nitrogen doublet by the proton phase change which is induced when the nitrogen pulse phase ϕ_1 is incremented by 90° (Pervushin et al., 1997).

Assuming a state of the density matrix ρ_a at point *a* as $-2H_zN_y$ for $\phi_1 = x$ and as $2H_xN_x$ for $\phi_1 = y$, chemical shift and J-coupling evolution will lead to a density matrix ρ_b at point *b* as:

$$\rho_b(\phi_1 = x) = -N_yH_\alpha \cos((\omega_N + \pi J)t_1)$$

$$+N_xH_\alpha \sin((\omega_N + \pi J)t_1) + N_yH_\beta \cos((\omega_N - \pi J)t_1)$$

$$-N_xH_\beta \sin((\omega_N - \pi J)t_1) \quad (2a)$$

$$\rho_b(\phi_1 = y) = N_x H_\alpha \cos((\omega_N + \pi J)t_1)$$
$$+N_y H_\alpha \sin((\omega_N + \pi J)t_1) - N_x H_\beta \cos((\omega_N - \pi J)t_1)$$
$$-N_y H_\beta \sin((\omega_N - \pi J)t_1) \quad (2b)$$

In order to perform simultaneous quadrature detection and separation of the upfield and downfield components of the nitrogen multiplet four FIDs with the following phase settings for ϕ_1, ϕ_2, and ϕ_3 are recorded for every t_1-increment (I: x,−y,−x; II: y,−y,−x; III: x,y,x; IV: y,y,x). A straightforward calculation using the results of Equations 1b and c shows that the usual cosine- and sine-modulated signals in t_1 and t_2 can be obtained from suitable linear combinations of these FIDs:

$$-(I + III)_x - (II - IV)_y = [(s^2 + s)\cos((\omega_N + \pi J)t_1)$$
$$-(s^2 - s)\cos((\omega_N - \pi J)t_1)]\cos(\omega_H t_2) \quad (3a)$$
$$(II + IV)_x - (I - III)_y = [(s^2 + s)\sin((\omega_N + \pi J)t_1)$$
$$-(s^2 - s)\sin((\omega_N - \pi J)t_1)]\cos(\omega_H t_2) \quad (3b)$$
$$(I + III)_x - (II - IV)_y = [(s^2 + s)\cos((\omega_N - \pi J)t_1)$$
$$-(s^2 - s)\cos((\omega_N + \pi J)t_1)]\cos(\omega_H t_2) \quad (3c)$$
$$-(II + IV)_x - (I - III)_y = [(s^2 + s)\sin((\omega_N - \pi J)t_1)$$
$$-(s^2 - s)\sin((\omega_N + \pi J)t_1)]\cos(\omega_H t_2) \quad (3d)$$

where subscripts x and y correspond to data points in the x- and y-channel of the proton receiver. The corresponding signals modulated by $\sin(\omega_H t_2)$ are obtained by rotating the receiver phases by 90° in Equation 3. For $s = 1$, i.e. $T = 1/(4J)$, Fourier transform of the linear combinations of Equations 3a and b and of Equations 3c and d will yield two subspectra containing only the upfield or downfield nitrogen singlets.

For $s = 1$, the amplitude of the signals equals 2 in Equation 3. However, as four FIDs have to be coadded the noise is increased by a factor of 2 as compared to one FID. Note that the reverse INEPT step of a normal ^{15}N-decoupled HSQC sequence transforms a coherence of type $2N_yH_z$ into a proton signal H_x. Therefore, the signal-to-noise ratio is the same for a normal HSQC singlet and for the upfield and downfield components obtained from the new doublet-separated sequence. However, in the doublet-separated scheme a loss in signal to noise per unit time of $\sqrt{2}$ results as twice the number of FIDs have to be recorded per complex t_1-increment. For the recently published IPAP scheme (Ottiger et al., 1998), the amplitude of each doublet component is half of the peak amplitude in a ^{15}N-decoupled HSQC. Therefore its sensitivity is a factor of $\sqrt{2}$ smaller compared to the new sequence. Conventional water-flip-back pulses were incorporated at appropriate points in the sequence of Figure 1 to further increase the sensitivity for fast exchanging amide protons (Grzesiek and Bax, 1993; Stonehouse et al., 1994). As the scheme in Figure 1 performs both **D**oublet **S**eparation and **S**ensitivity **E**nhancement, we refer to it as DSSE-HSQC.

Large variations in one-bond couplings result from the contribution of the residual dipolar couplings. The condition $T = 1/(4J)$, $s = 1$ is therefore rarely fulfilled. As a result, the second component of the doublet is not completely suppressed in Equation 3. The intensity ratio of this component over the selected component is $(1 - s)/(1 + s)$. Thus for small deviations $\Delta J = J - 1/(4T) << 1/(2\pi T)$, this ratio equals approximately $(2\pi\Delta JT)^2/4$. The suppression is therefore the same as in the non-enhanced IPAP sequence (Ottiger et al., 1998).

The discussion so far has neglected relaxation effects. As pointed out by Ottiger et al. (1998), the differential relaxation of doublet components due to dipolar/CSA interference is usually of little concern for proteins during the short reverse INEPT steps between time points *b* and *c*. A more serious source of error are the different lifetimes of transverse N_y and the $2H_yN_x$ coherences during the first reverse INEPT step between time points *b* and *c* (Equations 1b and c). In non-deuterated proteins, the $2H_yN_x$ coherence has a considerably shorter lifetime than the N_y magnetization. This is due to strong proton-proton dipolar relaxation and proton-proton J-couplings. The relative loss due to these mechanisms can be incorporated into Equation 1b (and into Equation 1d) by scaling the right-hand side with a loss factor *r*. As only signals resulting from terms in Equations 1b and c contribute to observable magnetization, it is easily seen that besides an overall factor r^2, this additional loss *r* has the same effect as changing *s* to *s/r*. The net effect is an incomplete suppression of the non-selected doublet component with an intensity ratio to the selected component of $(1 - s/r)/(1 + s/r)$. For a typical difference in loss rates between the N_y and the $2H_yN_x$ coherences of 50 Hz and for $T = 2.7$ ms, the incomplete suppression due to this loss is approximately −13%. In cases where the loss factor *r* and the incomplete suppression are uniform, such artifacts can be removed by a suitable linear combination with the spectrum of the non-selected component.

The pulse scheme is demonstrated for samples of the hepatitis C protease (comprising residues 1–180 of hepatitis C (strain BK) non-structural protein NS3 with an additional N-terminal methionine and an additional C-terminal ASKKKK sequence) in complex with a peptide-like inhibitor (Barbato et al., unpublished results) and for ubiquitin. In order to derive structural information contained in the residual dipolar couplings of weakly aligned molecules, samples of the hepatitis C protease were prepared as an isotropic solution as well as in an anisotropic state where the weak alignment is induced in the magnetic field by the presence of DMPC/DHPC lipid bicelles (Sanders and Schwonek, 1992; Tjandra and Bax, 1997; Ottiger and Bax, 1998). Three samples of uniformly ^{15}N-enriched proteins were used: (I): 0.3 mM hepatitis C protease in complex with the inhibitor, 16 mM phosphate, 0.2% β-octylglucoside, 2.8% (w/v) DMPC/DHPC in a weight ratio of 3.1:1 (Ottiger and Bax, 1998), pH 6.6. (II): 0.8 mM hepatitis C protease in complex with the inhibitor, 20 mM phosphate, 0.3% β-octylglucoside, pH 6.6. (III): 1.5 mM human ubiquitin (VLI Research, Southeastern, PA), pH 4.7. Solutions of ∼220 μl (95% H_2O/5% D_2O) were placed in Shigemi microcells.

All measurements were carried out on a BRUKER DMX-600 spectrometer equipped with a standard 5 mm, triple-resonance, triple-gradient probe. The 2D DSSE ^{15}N-^{1}H spectra were collected with the following numbers of complex data points and acquisition times:100*, 60 ms (t_1) × 512*, 55 ms (t_2) for samples of the hepatitis C protease complex (37 °C) and 400*, 240 ms (t_1) × 700*, 76 ms (t_2) for ubiquitin (25 °C) respectively. Data processing and analysis were performed using the programs NMRPipe (Delaglio et al., 1995) and PIPP (Garrett et al., 1991).

Figure 2 shows small regions of the DSSE-^{15}N-^{1}H-HSQC spectrum of the 0.3 mM hepatitis C protease complex recorded in the aligned state with the pulse sequence of Figure 1 (total measuring time 16 h). The narrow downfield (Figure 2A) and the broader upfield (Figure 2B) components of the nitrogen doublet were separated according to the linear combinations of FIDs described by Equation 3. Suppression of the non-selected components was in all cases better than ∼15%, i.e. undetectable at the signal-to-noise level of the spectrum.

Figure 2C displays the one-bond ^{1}H-^{15}N residual dipolar couplings $^{1}D_{NH}$ for the hepatitis C protease complex calculated as the difference of doublet splittings recorded in the liquid crystalline aligned state (sample I) and in the isotropic state (sample II). A

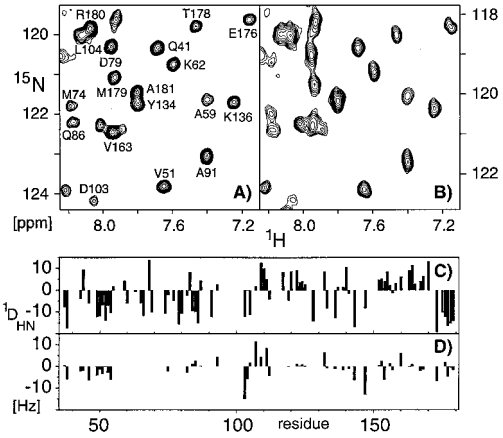

Figure 2. Data derived from the DSSE-^{15}N-^{1}H-HSQC recorded on the hepatitis C protease/inhibitor complex. (A,B): Selected regions of the DSSE subspectra (A: ^{15}N downfield, B: ^{15}N upfield) of the 0.3 mM hepatitis C protease complex recorded in the aligned state with the pulse sequence of Figure 1. (C) One-bond ^{1}H-^{15}N residual dipolar couplings $^{1}D_{NH,exp}$ for the hepatitis C protease complex. (D) Differences $^{1}D_{NH,exp} - {}^{1}D_{NH,X\text{-}ray}$ between measured ($^{1}D_{NH,exp}$) and calculated dipolar couplings ($^{1}D_{NH,X\text{-}ray}$) derived from PDB entry 1A1R.

total of 77 dipolar couplings are currently assigned ranging from ∼ −20 Hz to ∼10 Hz. This indicates that the alignment is comparable to the alignment of ubiquitin observed at approximately twofold higher concentration of the lipid bicelles (Tjandra and Bax, 1997).

Figure 2D depicts the differences in the observed dipolar couplings and the expected dipolar couplings calculated from a 2.5 Å X-ray structure of hepatitis C protease in complex with an activator peptide from the hepatitis C (strain H) non-structural protein NS4A (PDB entry 1A1R). An asymmetric alignment tensor was derived from a least squares fit of the X-ray coordinates to the observed dipolar splittings. Only non-mobile residues as identified by ^{15}N relaxation parameters ({^{1}H}-^{15}N NOE > 0.7, $R_{exchange} < 5$ Hz) were considered in the fit (N = 51). The rms deviation between the observed dipolar couplings and the calculated couplings is 4.8 Hz, whereas the rms of the measured dipolar couplings is 9.2 Hz. The NMR quality factor, defined as the ratio of these deviations (Cornilescu et al., 1998), is 0.52, thus indicating that there are substantial differences between the solution structure and the X-ray coordinates. Part of these structural differences are due to some of the highly conservative substitutions of amino acids between the two protease constructs. Another part of these deviations is expected from crystal packing artifacts and

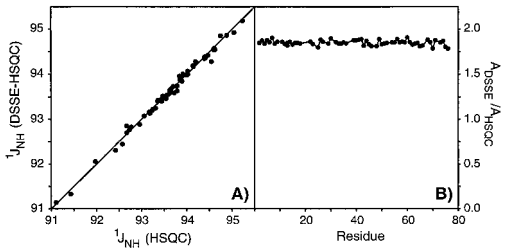

Figure 3. (A) Comparison of one-bond ^{1}H-^{15}N splittings for ubiquitin derived from the DSSE-HSQC (Figure 1) and a conventional water-flip-back HSQC without a proton decoupling pulse in the nitrogen evolution period. Both experiments were carried out under identical conditions, i.e. same number of complex data points, acquisition times and identical experimental time (1 h). Two (DSSE-HSQC) or four (conventional HSQC) scans were recorded for every single FID. (B) ratios of the peak amplitudes of the ^{15}N downfield components derived from the DSSE- HSQC and the conventional HSQC spectrum recorded under the conditions of Figure 3A.

from the structural differences induced on the protease upon binding to two highly different ligands, i.e. the inhibitor (NMR data) and the activator peptide (X-ray data). The three largest deviations ($>$10 Hz) stem from residues D103, V107 and S147 which are involved in crystal packing and in the ligation of the NS4A peptide. Despite these deviations, the correlation coefficient between the observed and calculated splittings is 0.85.

In order to test the precision of the splittings derived from the DSSE-HSQC experiment, their values were compared to splittings derived from a ^{1}H-coupled HSQC. Figure 3A shows $^1J_{HN}$ couplings for ubiquitin in the isotropic state derived from both methods. The agreement between both data sets is excellent as indicated by a pairwise root-mean-square difference of 0.07 Hz. Assuming the same statistical errors in both measurements, the precision of the individual DSSE measurement is therefore 0.05 Hz. Besides systematic errors stemming from the mentioned relaxation effects and pulse imperfections, the relaxation rates of the transverse nitrogen coherences $N_{x,y}H_\alpha$ and $N_{x,y}H_\beta$ limit the achievable precision in the DSSE experiment. For the hepatitis C protease complex at 37 °C the isotropic rotational correlation time is approximately 10.1 ns, i.e. about 2.5 times longer than for ubiquitin at 25 °C. The transverse nitrogen relaxation rates for the hepatitis C protease complex are therefore approximately 2.5 times faster. Assuming that the precision of 0.05 Hz for ubiquitin is purely limited by nitrogen relaxation rates, the achievable precision of the J-couplings in the DSSE experiment for the hepatitis C protease is expected to be about 0.13 Hz. As the range of the observed residual dipolar splittings in Figure 2C is two orders of magnitude larger than this value, the achievable precision of the DSSE-HSQC experiment is highly sufficient.

Figure 3B illustrates the sensitivity gain of the DSSE experiment versus a conventional ^{1}H coupled HSQC with water flip-back (Grzesiek and Bax, 1993). The ratios of peak amplitudes in both experiments carried out with the same total experimental time for the ubiquitin sample have a mean value of 1.84 (Figure 3B) and 1.87 for the ^{15}N downfield and upfield components, respectively. This corresponds to a loss of $\sim$7.5% as compared to the theoretical value of 2 not taking into account relaxation. As explained, this loss is dominated by the fast decay of the proton-nitrogen zero and double quantum magnetization present in the first reverse INEPT step of the TROSY (Equation 1b). The loss also includes effects of pulse imperfections and a less complete refocusing of the water magnetization. As expected, the rms value of the noise in one single DSSE subspectrum is 1.407 or $\sim\sqrt{2}$ larger than in the water-flip-back ^{1}H-coupled HSQC. The total sensitivity gain is therefore 1.31 and close to the theoretical value of $\sqrt{2}$.

Pervushin et al. (1998) have shown that not only ^1H_z, but also $^{15}N_z$ Boltzmann magnetization at the beginning of the TROSY pulse sequence contributes to the observable magnetization during the proton detection period. Depending on the relative phases of proton and nitrogen pulses during the first INEPT step, the downfield and the upfield components of the ^{1}H-^{15}N doublet are either enhanced or decreased by this $\sim$10–20% contribution of the ^{15}N Boltzmann population. On the Bruker DMX instrument, the choice of relative phases in Figure 1 has the advantage that the broader and therefore weaker upfield nitrogen resonance is enhanced whereas the narrow downfield resonance is reduced in its intensity.

In cases where the destructive interference of dipolar and CSA relaxation mechanisms leads to a narrowing of one of the components of the proton doublet, it might be desirable to detect only the narrow ^{1}H upfield component and correlate it to either the upfield or downfield component of the ^{15}N doublet. This can be achieved by omitting the heteronuclear decoupling scheme during data acquisition in the pulse scheme of Figure 1 and applying the last nitrogen 90° pulse ($\phi_4 = -x$). The sequence is then identical to the generalized TROSY (Andersson et al., 1998b) and correlates the narrow nitrogen component with

the narrow proton component and the broad nitrogen component with the broad proton component in a one-to-one fashion. If the signal from the broad proton component is too weak or too broad for analysis of the coupling constants, it is necessary to record a second data set where the broad nitrogen component is correlated to the narrow proton component. A phase change of ϕ_4 from $-x$ to $+x$ achieves the required inverse correlation by interchanging nitrogen $|\alpha>$ and $|\beta>$ spin states during the proton detection period. As twice the number of FIDs have to be recorded, a loss in sensitivity of $\sqrt{2}$ results compared to the DSSE-HSQC sequence. However, part of this loss could be regained if the Boltzmann ^{15}N component is used in a way that both the upfield and the downfield components are enhanced when they are selected in the respective subexperiments.

The achievable gain from the reduction of the proton linewidth during detection strongly depends on the relative contribution of the proton CSA and proton/nitrogen dipolar interaction to the total proton linewidth. In the case of an 85%–90% uniformly deuterated, ^{15}N-labelled sample of HIV-1 Nef (residues 39–206, Grzesiek et al., 1995) at 14 T magnetic field strength and 35 °C, the difference in linewidth between the upfield and downfield components of the proton doublet is about 30% as measured from the line shape of the proton doublet separated HSQC. This difference in linewidth is much smaller than expected for an isolated ^{1}H-^{15}N spin system because ^{1}H-^{1}H dipolar interactions and chemical exchange contribute measurably to the relaxation of both proton doublet components (Ishima et al., 1998). In practice, this means that the sensitivity gain from the proton line narrowing for this sample does not compensate for the loss resulting from the detection of only one doublet component. Larger gains in sensitivity are however expected for higher levels of deuteration, lower contributions of proton chemical exchange to the linewidth and stronger magnetic fields where the cancellation of the local dipolar and CSA fields is more complete (Pervushin et al., 1997).

Acknowledgements

We thank Gaetano Barbato, Renzo Bazzo and Chiara Nardi for supplying us with samples of the hepatitis C protease complex and Nico Tjandra for programs. This work was supported by the Humboldt foundation (F.C.), the Australian NH&MRC C.J. Martin Fellowship (A.J.D.) and DFG grant GR1683/1-1.

References

Andersson, P., Nordstrand, K., Sunnerhagen, M., Liepinsh, E., Turovskis, I. and Otting, G. (1998a) *J. Biomol. NMR*, **11**, 445–450.

Andersson, P., Annila, A. and Otting, G. (1998b) *J. Magn. Reson.*, **133**, 364–367.

Bax, A. and Tjandra, N. (1997) *J. Biomol. NMR*, **10**, 289–292.

Bothner-By, A.A., Domaille, P.J. and Gayathri, C. (1981) *J. Am. Chem. Soc.*, **103**, 5602–5603.

Cavanagh, J. and Rance, M. (1990) *J. Magn. Reson.*, **88**, 72–85.

Cornilescu, G., Marquardt, J.L., Ottiger, M. and Bax, A. (1998) *J. Am. Chem. Soc.*, **120**, 6836–6837.

Czisch, M. and Boelens, R. (1998) *J. Magn. Reson.*, **134**, 158–160.

Delaglio, F., Grzesiek, S., Vuister, G.W., Zhu, G., Pfeifer, J. and Bax, A. (1995) *J. Biomol. NMR*, **6**, 277–293.

Ernst, R.R., Bodenhausen, G. and Wokaun, A. (1987) *Principles of Nuclear Magnetic Resonance in One and Two Dimensions*, Clarendon Press, Oxford, p. 445.

Fäcke, T. and Berger, S. (1996) *J. Magn. Reson.*, **A119**, 260–263.

Garrett, D.S., Powers, R., Gronenborn, A.M. and Clore, G.M. (1991) *J. Magn. Reson.*, **95**, 214–220.

Grzesiek, S. and Bax, A. (1993) *J. Am. Chem. Soc.*, **115**, 12593–12594.

Grzesiek, S., Wingfield, P., Stahl, S., Kaufman, J.D. and Bax, A. (1995) *J. Am. Chem. Soc.*, **117**, 9594–9595.

Ishima, R., Wingfield, P T., Stahl, S.J., Kaufman, J. and Torchia, D.A. (1998) *J. Am. Chem. Soc.*, **120**, 10534–10542.

Kay, L.E., Keifer, P. and Saarinen, T. (1992) *J. Am. Chem. Soc.*, **114**, 10663–10665.

Meissner, A., Duus, J.Ø. and Sørensen, O.W. (1997a) *J. Magn. Reson.*, **128**, 92–97.

Meissner, A., Duus, J.Ø. and Sørensen, O.W. (1997b) *J. Biomol. NMR*, **10**, 89–94.

Ottiger, M., Delaglio, F. and Bax, A. (1998) *J. Magn. Reson.*, **131**, 373–378.

Ottiger, M. and Bax, A. (1998) *J. Biomol. NMR*, **12**, 361–372.

Palmer, A.G., Cavanagh, J., Wright, P.E. and Rance, M. (1991) *J. Magn. Reson.*, **93**, 151–170.

Pervushin, K., Riek, R., Wider, G. and Wüthrich, K. (1997) *Proc. Natl. Acad. Sci. USA*, **94**, 12366–12371.

Pervushin, K., Wider, G. and Wüthrich, K. (1998) *J. Biomol. NMR*, **12**, 345–348.

Ram, P. and Prestegard, J.H. (1988) *Biochim. Biophys. Acta*, **940**, 289–294.

Ross, A., Czisch, M. and Holak, T. (1996) *J. Magn. Reson.*, **A118**, 221–226.

Sanders, C.R. and Schwonek, J.P (1992) *Biochemistry*, **31**, 8898–8905.

Saupe, A. and Englert, G. (1963) *Phys. Rev. Lett.*, **11**, 462–465.

Stonehouse, J., Shaw, G.L., Keeler, J. and Laue, E.D. (1994) *J. Magn. Reson.*, **A107**, 178–184.

Tjandra, N. Grzesiek, S. and Bax. A. (1996) *J. Am. Chem. Soc.*, **118**, 6264–6272.

Tjandra, N. and Bax. A. (1997) *Science*, **278**, 1111–1114.

Tolman, J.R., Flanagan, J.M., Kennedy, M.A. and Prestegard, J.H. (1995) *Proc. Natl. Acad. Sci. USA*, **92**, 9279–9283.

Tolman, J.R. and Prestegard, J.H. (1996) *J. Magn. Reson.*, **B112**, 245–252.

Vold, R.R. and Prosser, P.S. (1996) *J. Magn. Reson.*, **B113**, 267–271.